Research Article | Vol. 26, No. 5 | 5 Mar 2018 | OPTICS EXPRESS 6158
Optics EXPRESS

Dimensioning of a multibeam coherent photonic beamformer fed by a phased array antenna

MIGUEL V. DRUMMOND,[1,*] VANESSA C. DUARTE,[1,2] ANDRÉ ALBUQUERQUE,[1] ROGÉRIO N. NOGUEIRA,[1,3] LEONTIOS STAMPOULIDIS,[4] GEORG WINZER,[5] LARS ZIMMERMANN,[5] STEPHEN CLEMENTS,[6] AND JAVAD ANZALCHI[7]

[1] *Instituto de Telecomunicações, Universidade de Aveiro, 3810-193 Aveiro, Portugal*
[2] *Department of Physics, University of Aveiro, 3810-193, Aveiro, Portugal*
[3] *Watgrid, Lda., Campus Universitário de Santiago 3810-193 Aveiro, Portugal*
[4] *Gooch and Housego, Systems Technology Group, Broomhill Way, Torquay, Devon, TQ2 7QL, UK*
[5] *IHP, 15236 Frankfurt, Germany*
[6] *aXenic, Durham, UK*
[7] *Airbus Defence and Space, Telecommunications Satellites Business Division, Stevenage, UK*
[*] *mvd@av.it.pt*

Abstract: The design and dimensioning of a photonic-aided payload for a multi-beam high-throughput communications satellite is a complex problem in which the antenna, RF and photonic subsystems must be considered as a whole for achieving best performance with lowest mass and power consumption. In this paper, we propose and dimension the receiving stage of a communications satellite comprising a phased array antenna (PAA) feeding a multibeam photonic beamforming system (PBS). The PBS uses a single wavelength and resorts to heterodyne detection such that the retrieved beams are frequency downconverted. End-to-end system modeling shows that the complexity of the PAA and PBS can be traded-off for signal-to-noise ratio (SNR) or power consumption without compromising the beam width. The dimensioning of a realistic scenario is presented, showing that an SNR and beam crosstalk on the order of 20 dB are achievable with a total power consumption below 1 kW for a typical number of 100 antenna elements (AEs).

OCIS codes: (060.5625) Radio frequency photonics; (280.5110) Phased-array radar.

References and links

1. P. Inigo, O. Vidal, B. Roy, E. Alberty, N. Metzger, D. Galinier, J. Anzalchi, G. Huggins, and S. Stirland, "Review of terabit/s satellite, the next generation of HTS systems," in *Advanced Satellite Multimedia Systems Conference and the 13th Signal Processing for Space Communications Workshop (ASMS/SPSC)* (2014), pp. 318-322.
2. F. Khan, "Mobile internet from the heavens," arXiv:1508.02383, 2015.
3. J. Anzalchi, P. Inigo, and B. Roy, "Application of photonics in next generation telecommunication satellites payloads," Proc. SPIE **10563**, 1056330 (2017).
4. E. Chen and A. Murphy, *Broadband Optical Modulators: Science, Technology, and Applications* (CRC, 2011).
5. M. Kechagias, J. Crabb, L. Stampoulidis, J. Farzana, E. Kehayas, M. Filipowicz, M. Napierala, M. Murawski, and T. Nasilowski, "Multi-core fiber amplifier array for intra-satellite links," Proc. SPIE 10562, 1056258 (2016).
6. G. Winzer, M. Kroh, S. Lischke, D. Knoll, K. Voigt, H. Tian, C. Mai, D. Petousi, D. Micusik, L. Zimmermann, B. Tillack, and K. Petermann, "Monolithic photonic-electronic QPSK receiver for 28Gbaud," in *Optical Fiber Communication Conference*, OSA Technical Digest (online) (Optical Society of America, 2015), paper M3C.4.
7. V. C. Duarte, M. V. Drummond, and R. N. Nogueira, "Photonic True-Time-Delay Beamformer for a Phased Array Antenna Receiver based on Self-Heterodyne Detection," J. Lightwave Technol. **34**, 5566-5575 (2016).
8. C. Roeloffzen, R. Oldenbeuving, R.B. Timens, P. van Dijk, C. Taddei, A. Leinse, M. Hoekman, R.G. Heideman, L. Zhuang, D. Marpaung, and M. Burla, "Integrated Optical Beamformers," in *Optical Fiber Communication Conference*, OSA Technical Digest (online) (Optical Society of America, 2015), paper Tu3F.4.
9. Maurizio Burla, David A.I. Marpaung, Leimeng Zhuang, Muhammad Rezaul Khan, Arne Leinse, Willem Beeker, Marcel Hoekman, René G. Heideman, and Chris G.H. Roeloffzen, "Multiwavelength-Integrated Optical Beamformer

#315706 https://doi.org/10.1364/OE.26.006158
Journal © 2018 Received 14 Dec 2017; revised 6 Feb 2018; accepted 9 Feb 2018; published 28 Feb 2018

Optics EXPRESS

Based on Wavelength Division Multiplexing for 2-D Phased Array Antennas," J. Lightwave Technol. **32**, 3509–3520 (2014).
10. A. Meijerink, C. G. H. Roeloffzen, R. Meijerink, L. Zhuang, D. A. I. Marpaung, M. J. Bentum, M. Burla, J. Verpoorte, P. Jorna, A. Hulzinga, and W. van Etten, "Novel Ring Resonator-Based Integrated Photonic Beamformer for Broadband Phased Array Receive Antennas—Part I: Design and Performance Analysis," J. Lightwave Technol. **28**, 3–18 (2010).
11. L. Zhuang, C. G. H. Roeloffzen, A. Meijerink, M. Burla, D. A. I. Marpaung, A. Leinse, M. Hoekman, R. G. Heideman, and W. van Etten, "Novel Ring Resonator-Based Integrated Photonic Beamformer for Broadband Phased Array Receive Antennas—Part II: Experimental Prototype," J. Lightwave Technol. **28**, 19–31 (2010).
12. S. Pan, D. Zhu, S. Liu, K. Xu, Y. Dai, T. Wang, J. Liu, N. Zhu, Y. Xue, and N. Liu, "Satellite Payloads Pay Off," Microwave Magazine **16**(8), 61–73 (2015).
13. H. Wolf, M. Schneider, S. Stirland, and D. Scouarnec, "Satellite multibeam antennas at airbus defence and space: State of the art and trends," *European Conference on Antennas and Propagation* (EuCAP, 2014), pp. 182–185.
14. V.J. Urick, "Considerations and Application Opportunities for Integrated Microwave Photonics," in Optical Fiber Communication Conference, OSA Technical Digest (online) (Optical Society of America, 2016), paper M2B.1.
15. R. C. Hansen, *Phased Array Antennas* (John Wiley and Sons, 2009).
16. J.J. Lee, "G/T and noise figure of active array antennas," IEEE Trans. Antennas Propagation **41**(2), 241–244 (1993).
17. J. R. Adleman, C. L. Lin, S. B. Jester, B. Melvin Pascoguin, D. C. Evans, and E. W. Jacobs, "Photonic RF-IF wideband down conversion using optical injection locking," Proc. SPIE **9467**, 946721 (2015).
18. V. C. Duarte, M. V. Drummond, and R. N. Nogueira, "Photonic true-time delay beamforming system for a phased array antenna receiver," *2015 SBMO/IEEE MTT-S International Microwave and Optoelectronics Conference* (IMOC, 2015), pp. 1-5.
19. V. Duarte, J. Prata, C. Ribeiro, R. Nogueira, G. Winzer, L. Zimmermann, R. Walker, S. Clements, M. Filipowicz, M. Napierala, T. Nasilowski, J. Crabb, L. Stampoulidis, J. Anzalchi, and M. Drummond, "Integrated photonic true-time delay beamformer for a ka-band phased array antenna receiver," in *Optical Fiber Communication Conference*, OSA Technical Digest (online) (Optical Society of America, 2018), paper M2G.5.

1. Introduction

High-throughput communications satellites are an elegant solution for providing ubiquitous wireless broadband access to a large number of users, as a single system is able to cover entire continents with multiple spot beams [1, 2]. Communications satellites currently face two main challenges. First, the ever-increasing bandwidth demand is pushing for an increase in number and density of beams. Second, given the wide coverage of a communications satellite, the geographic distribution of bandwidth demand changes over the lifetime of a satellite, thus requiring flexible coverage. Consequently, the ultimate goal is to develop a software-defined high-capacity satellite.

Without technology improvement, the required increase in capacity and flexibility unavoidably increases satellite payload mass and power consumption. However, the currently used RF payload, albeit mature and reliable, is fairly static and reaching its limits, and thus there is an emergent need for a technology leap. Photonics has been identified as a disruptive technology able to provide at least the same functionality as RF payloads, but with reduced mass and power consumption, and with increased flexibility [3]. An intense effort has been made to improve photonic components and subsystems, namely modulators [4], optical amplifiers (OAs) [5], detectors [6] and beamformers [7–11]. However, there has been little discussion on how to introduce photonic components and subsystems to smoothly replace the current RF payload [3, 12], unfortunately not even providing a quantitative dimensioning of the complete payload. Therefore, the objective of this paper is to provide, for the first time to the authors knowledge, end-to-end system modeling and dimensioning of the receiving stage of a payload, comprising a PAA feeding a multibeam PBS, whose main objective is to resemble a typical RF heterodyne receiver.

This paper is structured as follows. Section 2 briefly introduces a satellite link, focusing on key specifications of beams. Section 3 presents the proposed multibeam coherent photonic beamformer, and explains the motivation behind its design. Section 4 presents a beam distortion analysis of the proposed PBS in a realistic scenario. The impact of array thinning and suitability of true-time delay (TTD) beamforming are assessed in terms of beam width, crosstalk and squinting. Section 5 presents a noise model of the proposed PBS which includes all significant electrical and optical noise sources, allowing to estimate the output power and SNR. Section 6

Optics EXPRESS

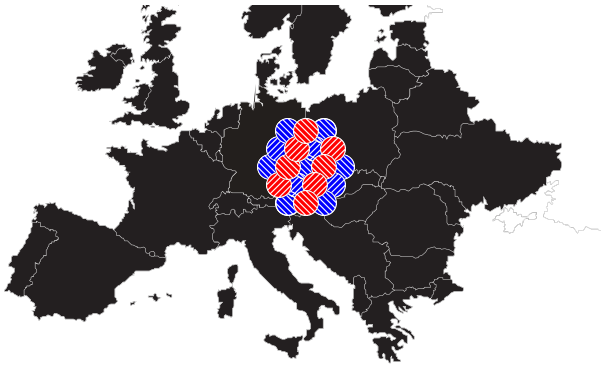

Fig. 1. User beams with four different colors spread across center Europe.

presents a simple estimation of the power consumed by each stage of the system. Section 7 takes the tools presented in sections 4 to 6 to dimension the complete system as a function of SNR, power consumption and beam crosstalk. Section 8 presents the final conclusions.

2. Satellite link

A communications satellite relays information between gateways and users, in which gateways are typically connected to the World Wide Web, thereby providing Internet access to users [1]. Thus, a satellite link comprises four links, which are forward and return gateway and user links. While a few gateways serve a large number of users, users are spread across wide areas. Hence, the satellite must handle a large number of user links, each of which defines a user beam. The total capacity of the satellite is therefore proportional to the spectral width attributed to each user beam, and to the number of user beams [1].

There are two basic guidelines in dimensioning the satellite payload such that all user beams can be provisioned. First, the frequency of uplink user signals should be higher than that of downlink user signals. The reason is that it is simpler for the satellite to generate high-power downlink signals at lower frequencies. On top of this, with the exception of attenuation peaks, lower frequency signals suffer lower atmospheric attenuation. Second, in order to avoid crosstalk among adjacent beams, these are given different colors, i.e., different frequencies and/or polarization. This is depicted in Fig. 1, in which a frequency reuse scheme comprising four colors is depicted. In such scheme two adjacent beams have the same frequency or polarization, but not both.

Therefore, it is safe to state that the most challenging satellite link to address is the user uplink, as the receiver processes input signals with high carrier frequency, various colors, very low power, and spread over a vast region, and outputs a high number of user beams.

3. Coherent photonic beamformer

The first stage of the multibeam receiver is the antenna receiver. Therefore, it is important to choose a suitable antenna architecture for the envisaged scenario. There are essentially three multibeam antenna architectures: single feed per beam (SFB), multiple feeds per beam (MFB) and active array (AA) antennas [13]. SFB antennas take a given set of AEs, referred to as a feed, and perform fully passive and thus static beamforming previously to low-noise amplification, outputting a single beam. While conceptually simple, SFB antennas are inflexible and unsuitable for a large number of beams. Stepping up to MFB antennas decreases the number of feeds as these are shared to beamform multiple beams, thus improving scalability. However, only one amplifier per beam is still used, which implies that beamforming is static as well. Such limitation

Optics EXPRESS

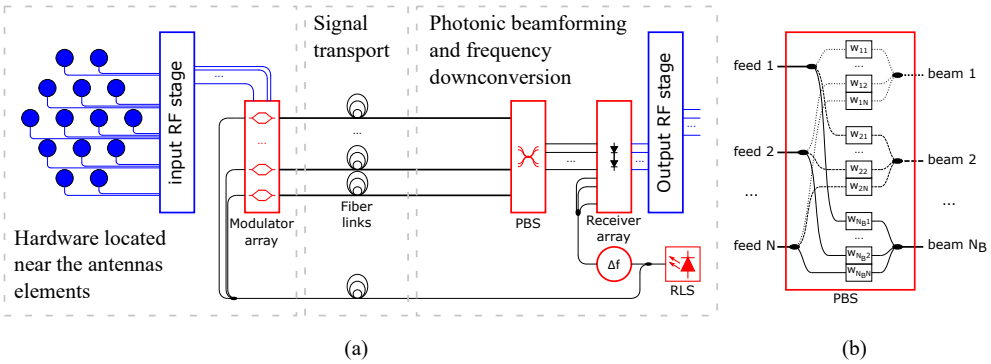

Fig. 2. (a) scheme of the proposed receiving stage. (b) detailed PBS with N feeds producing N_B output beams, and tuned by $N \times N_B$ phase shifters with a complex weight of w_{bn}.

vanishes when using AA antennas, as each feed is connected directly to one amplifier, such that beamforming is dynamically performed after the amplification stage. Such antennas thus are basically PAAs. Consequently, AA antennas enable a large number of beams, thus being suitable for the targeted high-capacity and flexible coverage.

Current RF payloads rely on coherent combination of signals followed by heterodyne detection such that uplink signals are frequency-downconverted into downlink beams [3]. In order to smoothly transition from RF to photonic-aided payloads, the proposed receiving stage, depicted in Fig. 2, follows the same rationale. The PAA comprises horn AEs, which are typically disposed in an hexagonal lattice [13]. The AEs feed the input RF stage, which forms the feeds such that one feed results from the contribution of at least one AE. Without loss of generality, it is assumed herein that each feed comprises a single AE. The input RF stage also provides low-noise amplification to each feed. The amplified feed signals are then converted to optical signals by means of an array of electro-optic modulators (EOMs) providing amplitude modulation. Each modulator may thus be a Mach-Zehnder modulator (MZM) biased at the minimum transmission point. Given that the main objective of the proposed receiving stage is to resemble a typical RF architecture, all optical signals originate from a single reference laser source (RLS) [7], and are transported to the PBS through very short fiber links without resorting to wavelength-division multiplexing. The PBS is essentially a coherent multiple-input multiple-output (MIMO) processor that separates the various beams from the input optical signals, thus comprising N_B beamforming stages. Such system is detailed in the next section. In addition, as explained in section 5, optical amplification can be included in different parts of the system. Each beamformed optical signal is converted to a frequency-downconverted RF signal by means of heterodyne detection. In order to avoid laser phase noise through phase noise cancellation, a frequency-shifted (Δf) optical local oscillator (FSOLO) is generated from the RLS, thus resulting in self-heterodyne detection [7]. The output RF stage provides electrical amplification and filtering and, if required, further RF frequency downconversion.

The main advantage of any photonic payload is that signal transport resorts to optical fibers, which are less lossy and much lighter than coaxial cables. Nonetheless, the proposed system has additional advantages. First, optical amplification is not saturated by a strong optical carrier, given its suppression due to amplitude modulation. Second, thanks to heterodyne detection, RF phase shifting is equivalent to optical phase shifting [7]. Given that the PBS comprises waveguides, couplers and phase shifters, and that all of those have a size proportional to the operating wavelength, the PBS can be miniaturized by a factor of $\nu/f_{\mathrm{RF}} \approx 5000$, where $f_{\mathrm{RF}} = 30\,\mathrm{GHz}$ is the RF frequency and $\nu = 193.5\,\mathrm{THz}$ is the RLS frequency [14]. Such advantage confirms that the proposed system complies with a decrease of mass. Third, the proposed system requires

Optics EXPRESS

a few different colorless optical devices, enabling the use of cost-effective device arrays and simplifying the provisioning of redundant hardware for failure protection.

4. Beam distortion analysis

The PAA and the PBS form a MIMO system with up to N input feeds and as many outputs as the number of beams, N_B, which provides spatial filtering and thus beam separation [15]. The filter transfer function for beam b is given by

$$Y_b(\theta,\phi) = R(\theta,\phi)F_b(\theta,\phi) = R(\theta,\phi)\sum_{n=1}^{N} w_{bn}e^{-j\boldsymbol{k}\cdot\boldsymbol{r}_n}, \tag{1}$$

where $R(\theta,\phi)$ is the radiation pattern of each AE as a function of the spherical coordinates θ and ϕ, $F_b(\theta,\phi)$ is the array factor for beam b, $\boldsymbol{k}$ is the wave vector of the incident wave given by $\boldsymbol{k} = \frac{\omega}{c}(\sin(\theta)\cos(\phi), \sin(\theta)\sin(\phi), \cos(\theta))$ and $\boldsymbol{r}_n = (x_n, y_n, z_n)$ are the coordinates of the n^{th} AE.

The task of the PBS is to define the filter taps w_{bn}. The flexibility of the PBS depends on whether such taps are adjustable. If so, then $F_b(\theta,\phi)$ may point to any desired direction, thus providing full flexibility. The phase of w_{bn} can be constant or proportional to the frequency ω. If constant, a single optical phase shifter can be used to tune the phase. However, in this case, $F_b(\theta,\phi)$ becomes frequency dependent. This behavior is usually referred to as beam squinting [15]. If beam squinting is too significant, the phase of w_{bn} should be made proportional to the frequency ω, and thus a tunable optical delay line (TODL) is also needed besides the optical phase shifter. Such case corresponds to TTD beamforming. Resorting solely to optical phase shifters thus leads to the smallest footprint. However, such is only possible if beam squinting is within acceptable limits. Before assessing beam squinting let us first define the simulation scenario and dimension the PAA.

4.1. Array thinning

In order to assess the impact of the spatial distribution of AEs and of having frequency-independent filter taps, let us assume the following simulation scenario based on [1,13]. The receiver processes $N_B = 260$ uplink user beams, each with a target half-power beam width (HPBW) of 0.21°, addressing the entire European continent, which, from the geostationary orbit, requires a horizontal vs. vertical steering range of $7° \times 4°$. The distance between two adjacent AEs is of $d = 2$ cm [13], and, for a matter of simplicity, $R(\theta,\phi) = 1$. The RF spectrum spans from 27.5 GHz to 30 GHz, in accordance with the frequency plan of the return user uplink proposed in [1]. Thus, an RF frequency of $f_{\text{RF}} = 28.75$ GHz is considered, which corresponds to the center frequency of such frequency plan. Figure 3(a) shows the obtained HPBW as a function of N. α and β are the scanning angles along the horizontal and vertical axes, such that $\phi = \tan^{-1}(\tan(\beta)/\tan(\alpha))$ and $\theta = \tan^{-1}(\tan(\alpha)/\cos(\phi))$. It is also assumed that $w_{bn} = 1, \forall n = 1,\ldots,N$. The HPBW decreases with the increase of the span of the PAA, which is proportional to N. The target HPBW requires at least $N = 19927$ AEs, spanning about $2 \times 2\,\text{m}^2$.

The number of AEs should be defined from specifications such as SNR, mass and power consumption, and not by the PAA span required to obtain a certain beam width. Such can be achieved by maintaining the PAA span while removing AEs, therefore resulting in a thinned array [15]. How to thin the array is a combinatorial optimization problem, whose objective is to minimize the side lobe power of the array factor. Nonetheless, the basic rule is that in order to avoid having multiple main lobes, repetitive procedures such as periodically removing one out of ten elements in a given direction should be avoided [15]. If so, thinning can be advantageously used to shape the array factor and thus control the side lobe power, thereby enabling w_{bn} to have

Optics EXPRESS

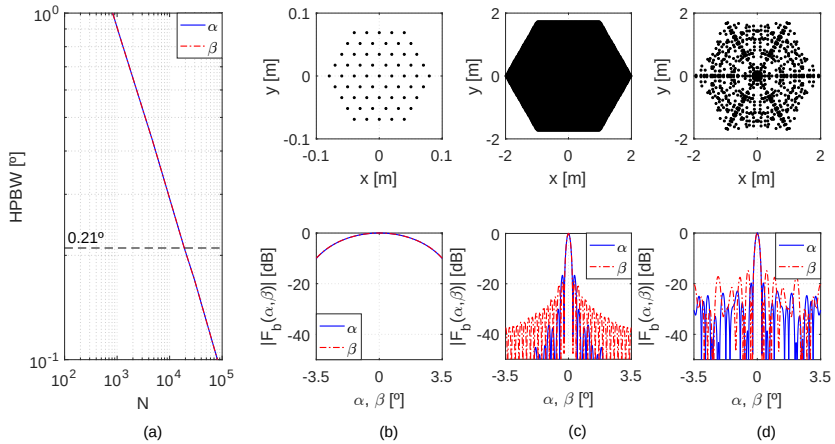

Fig. 3. (a) Horizontal (α) and vertical (β) HPBW as a function of the number of AEs. (b) - (d) top: spatial arrangement of the AEs for $N = 61$, $N = 19927$, and for a thinned array with $N = 1116$ AEs selected from the array at its left; bottom: corresponding array factors $|F_b(\alpha, 0)|$ and $|F_b(0, \beta)|$.

a constant absolute value. Consequently, without loss of generality, the PBS only needs to tune the phase of w_{bn}, leaving its absolute value constant.

Figure 3(d) considers a thinned array generated from the filled one at its left according to the simple rule that only the AEs complying with $\left|\frac{|r_n|}{d} - \left[\frac{|r_n|}{d}\right]\right| \leq 10\,\%$ such that $\left[\frac{|r_n|}{d}\right]$ is a prime number are included in the array, where $[x]$ is the nearest integer to x. While the main lobe remains identical, side lobes have been enhanced. Nonetheless, the maximum normalized side lobe power remains at -15 dB.

4.2. *Beam squinting and crosstalk*

Resorting to a thinned PAA does not change the phase or time delay differences among input signals that need to be compensated by the PBS, which therefore produces the same beam squinting as for a non-thinned array. In order to assess the relevance of beam squinting on the presented simulation scenario, let us consider the worst-case scenario in which the target beam has the widest arrival angles of $(\alpha_T, \beta_T) = (3.5°, 2.0°)$, and that the spectral width of the RF signal, B, may go up to 2.5 GHz. Let us also consider the thinned array shown in Fig. 3(d) with $|w_{bn}| = 1, \forall n = 1, \ldots, N$, and with optimized phase values, i.e., squint-free beamforming, for $f_{\mathrm{RF}} = 28.75$ GHz. The simulation results are shown in Fig. 4.

As expected, beam squinting increases proportionally to $\delta f = f - f_{\mathrm{RF}} = B/2$, reaching $(-0.15°, -0.08°)$ for $\delta f = 1.25$ GHz. Nonetheless, as the steering range and maximum fractional bandwidth, given by $B/f_{\mathrm{RF}} = 8.7\%$, are both small, the main lobe remains undistorted even for $\delta f = 1.25$ GHz. Such can be confirmed by comparing the array factors of Figs. 4(b) and 4(c), and by observing that the HPBW decreases negligibly with the increase of δf.

Even though beam squinting does not distort the main lobe, it leaks undesirable power from beams adjacent to the target beam having the same color, i.e., beam crosstalk. As shown in Fig. 4(b), thanks to the hexagonal lattice disposition of the AEs and to the used four color frequency reuse scheme, the adjacent beams with same color align almost perfectly with minima of the array factor, leading to a beam crosstalk below -25 dB. However, as shown in Fig. 4(c) top, such alignment vanishes due to beam squinting, and some adjacent beams become positioned near local maxima of the array factor, leading to a worst-case beam crosstalk of -16 dB.

Optics EXPRESS

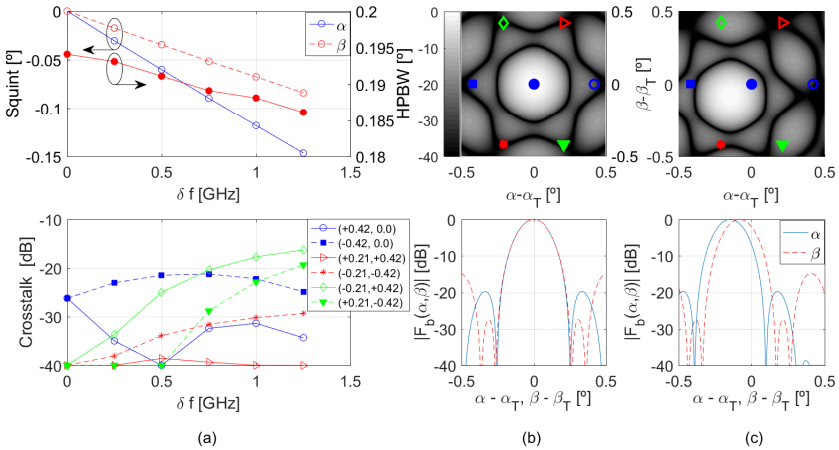

Fig. 4. (a) top: beam squinting and HPBW as a function of δf; bottom: crosstalk from nearest beams with the same color as a function of δf. (b) and (c) top: Magnitude (in dB) of the array factor centered at the target angle. The markers identify the angles of the nearest beams with the same color as the target beam. Bottom: corresponding array factors $|F_b(\alpha, \beta_T)|$ and $|F_b(\alpha_T, \beta)|$. (b) shows the results corresponding to $\delta f = 0$, whereas in (c) $\delta f = 1.25$ GHz.

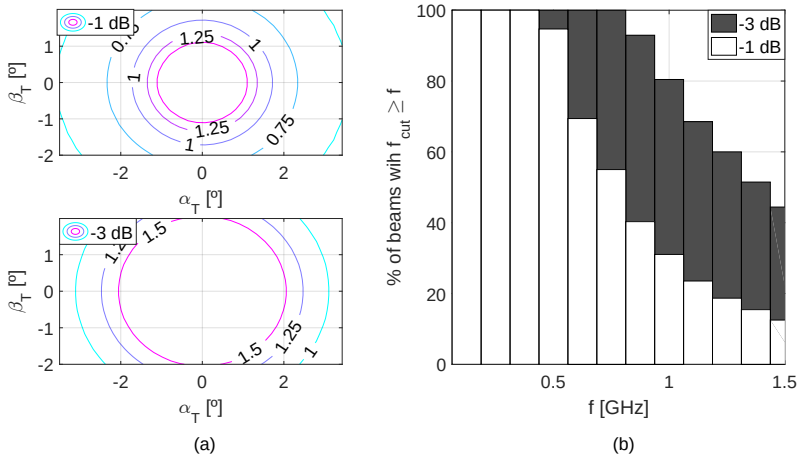

Fig. 5. (a) cutoff frequencies (in GHz) at -1 dB and -3 dB of $|F_b(\alpha, \beta)|$. (b) percentage of beams with a cutoff frequency of at least f, which can be interpreted as the percentage of beams with spectral width of $B = 2f$ that dispense TTD beamforming.

4.3. *Need for true-time delay beamforming*

While beam squinting leaks power from a given target beam into adjacent ones, thus affecting such beams, such power leaking affects the target beam as well. The proportional increase of beam squinting with frequency translates into a low-pass filtering effect on $|F_b(\alpha_T, \beta_T)|$, thus affecting the signal carried by a beam. Figure 5(a) displays the cutoff frequencies of $|F_b(\alpha_T, \beta_T)|$. The simulation scenario is the same as used above, however with the horizontal vs. vertical steering range fully filled by a total of 680 beams.

The cutoff frequency of the array factor decreases as the arrival angles increase, as the uncompensated time delay of signals generated by the outer AEs increases as well. The minimum

Optics EXPRESS

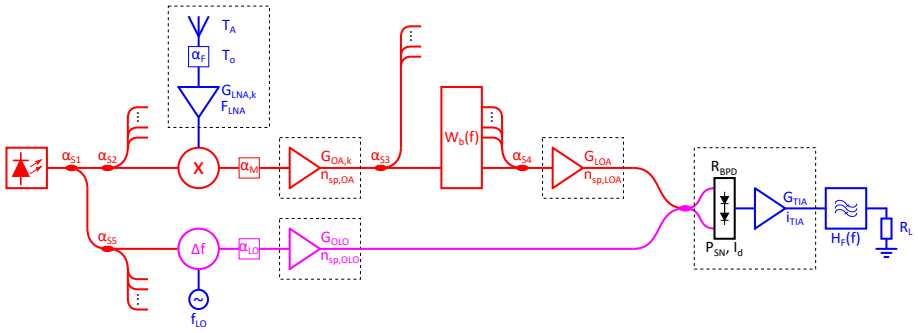

Fig. 6. Scheme of the photonic payload architecture for one output beam including noise sources.

cutoff frequencies at −1 dB and −3 dB are of 433 MHz and 772 MHz. Hence, beams with a spectral width up to 866 MHz have a frequency-dependent attenuation lower than 1 dB, and can be assumed as squint-free without requiring TTD beamforming. For the widest spectral width of 2.5 GHz, only about 18.7 % of the beams are in such condition.

For the remaining beams to be retrieved without beam squinting, TTD beamforming may be employed. If TTD beamforming is considered, the required tuning range for each AE and beam can be derived from (1), and is given by

$$\tau_n(\alpha_T, \beta_T) = \frac{\boldsymbol{k} \cdot \boldsymbol{r}_n}{\omega_{\mathrm{RF}}}. \tag{2}$$

For the widest arrival angles of $(\alpha_T, \beta_T) = (3.5°, 2.0°)$ the required value for the outermost AEs is of ±330 ps, decreasing in value towards the center AE down to 0 ps.

5. Noise model

As mentioned above, array thinning allows changing the number of AEs without affecting beam shape or squinting, leaving such parameter to be defined by SNR, mass and power consumption specifications. In this section, we derive the SNR of the proposed system. The proposed system can be detailed to include all relevant noise sources, thus allowing an accurate estimation of the output power and SNR. Such detailed scheme is presented in Fig. 6, addressing a single beam for the sake of clarity. The laser signal is shared by other AEs through the optical coupler α_{s2}. The contribution of a given AE to other output beams is provided through the optical coupler α_{s3}. The optical coupler α_{s4} combines all phase-shifted contributions into the output beam, whereas the optical coupler α_{s5} splits the laser signal by the N_B coherent receivers. The considered system model assumes distortionless devices, including EOMs and frequency shifters. The model includes all relevant noise sources with the exception of phase and intensity noise from the input laser source, the latter of which can be neglected when using balanced photoreceivers. As explained in [7], phase noise can be considered as canceled as long as the maximum delay between one of the signals and the FSOLO remains well below the coherence time of the laser, which is the inverse of its linewidth.

Let us assume that the input RF signals generated by all AEs are given by $v_k(t) = v(t) = a(t)\sin(\omega_{\mathrm{RF}}t + \theta(t))$, with $a(t)$ and $\theta(t)$ representing the amplitude and phase modulation and ω_{RF} the RF angular frequency. Such assumption already includes phase and time delay synchronization obtained by beamforming. For a matter of simplicity, let us also assume that the gains of the low-noise amplifiers (LNAs) as well as of the OAs set after modulation are identical, i.e., $G_{\mathrm{LNA,k}} = G_{\mathrm{LNA}}$ and $G_{\mathrm{OA,k}} = G_{\mathrm{OA}}$, and that the PBS only resorts to phase shifting, such that

Optics EXPRESS

$w_{bn}(f) = w_{bn}$. The output signal is given by

$$v_{\text{out}}(t) = 2P_{\text{L}}R_{\text{BPD}}G_{\text{TIA}}\sqrt{G_{\text{OBF}}G_{\text{TOLO}}} \cdot \frac{a(t)}{2}\sin\left(\Delta\omega t + \theta\left(t\right)\right) \cdot \sum_{n=1}^{N} w_{bn}, \tag{3}$$

where P_{L} is the power of the laser source, R_{BPD} is the responsivity of the balanced photodetector (BPD) and G_{TIA} is the transimpedance gain of the transimpedance amplifier (TIA). The gain constants of the signals and optical local oscillator (OLO) paths are given by $G_{\text{OBF}} = G_{\text{LNA}}G_{\text{OA}}G_{\text{LOA}}/(\alpha_{s1}\alpha_{s2}\alpha_{s3}\alpha_{s4}\alpha_{\text{F}}\alpha_{\text{M}})$ and $G_{\text{TOLO}} = G_{\text{OLO}}\left(\alpha_{s1} - 1\right)/(\alpha_{s1}\alpha_{s5}\alpha_{\text{LO}})$, where α_{sm} is the power splitting or combining factor of the m^{th} optical coupler, α_{F} is the antenna feed loss, and α_{M} models the modulation related losses of the EOM, combining insertion loss (IL) with the half-wave voltage of the EOM as $\alpha_{\text{M}} = \text{IL} \cdot V_{\pi}^{-2}$, which is a suitable approximation for low modulation indexes. Likewise, α_{LO} models the modulation related losses of the frequency shifter, G_{LOA} is the gain of the last optical amplifier (LOA) set after the PBS and G_{OLO} is the gain of the OA at the OLO path. The output signal is downconverted to a frequency of $\Delta\omega = \omega_{\text{RF}} - \omega_{\text{LO}}$, where ω_{LO} is the frequency shift given to the OLO. The amplitude of the signal is halved as the frequency upconverted term is filtered out by the output bandpass filter, whose transfer function $H_F(f)$ is centered at $\Delta\omega$, unitary within a given bandwidth such that the input signal does not suffer from narrowband filtering, and zero elsewhere. The average output signal power is thus given by

$$P_{\text{out}} = P_{\text{L}}^2R_{\text{BPD}}^2\frac{G_{\text{TIA}}^2}{R_L}G_{\text{OBF}}G_{\text{TOLO}} \cdot P_s \cdot \left(\sum_{n=1}^{N} w_{bn}\right)^2, \tag{4}$$

where R_L is the output load and P_s is the power of each input RF signal.

Let us now address the noise sources, assuming that all are i.i.d.. The contribution at the system output associated with all input RF signals is given by [16]

$$P_{\text{n,AE}} = P_{\text{L}}^2R_{\text{BPD}}^2\frac{G_{\text{TIA}}^2}{R_L}G_{\text{OBF}}G_{\text{TOLO}} \cdot (P_A + P_F + P_{\text{LNA}}) \cdot \sum_{n=1}^{N} w_{bn}^2, \tag{5}$$

where the antenna and feed noise contributions are respectively given by $P_A = k_BT_AB$ and $P_F = k_BT_o\left(\alpha_F - 1\right)B$, k_B is the Boltzmann constant, T_A is the noise temperature of each AE and T_o is the feed temperature. The LNA noise contribution is given by $P_{\text{LNA}} = \alpha_F k_B T_o(F_{\text{LNA}} - 1)B$, where F_{LNA} is the LNA noise figure.

The amplified spontaneous emission (ASE) noise contribution from the OAs is given by

$$P_{\text{n,OA}} = P_{\text{L}}R_{\text{BPD}}^2\frac{G_{\text{TIA}}^2}{R_L}G_{\text{TOLO}} \cdot 2\left(P_{\text{ASE,OA}}\frac{G_{\text{LOA}}}{\alpha_{s3}\alpha_{s4}}\sum_{n=1}^{N} w_{bn}^2 + P_{\text{ASE,LOA}}\right), \tag{6}$$

where $P_{\text{ASE,OA}} = n_{\text{sp,OA}}(G_{\text{OA}} - 1)h\nu B$ and $P_{\text{ASE,LOA}}$ has the same expression however with $n_{\text{sp,LOA}}$ and G_{LOA} instead, n_{sp} is the spontaneous emission factor and h is the Planck constant. It is assumed that the ASE noise is polarized and has the same state-of-polarization as the signal. In comparison with the noise power terms in (5), the ASE noise power is multiplied by 2. The noise sources in (5) have roughly the same spectral power distribution as the input RF signal, and thus also have half of their spectral content filtered out by the output bandpass filter. However, this is not the case of ASE noise, which has a wide uniform spectral power distribution. The noise added by the OLO OA can be neglected as even after amplification the SNR of the OLO is much higher than the one of the LOA output signal.

Optics EXPRESS

The contribution of the noise sources of the output stage, i.e., shot noise generated in the photodiodes, P_{SN}, and TIA amplification noise, P_{TIA}, is given by

$$P_{\mathrm{n,out}} = \frac{G_{\mathrm{TIA}}^2}{R_L} \cdot (P_{\mathrm{SN}} + P_{\mathrm{TIA}}) \approx \frac{G_{\mathrm{TIA}}^2}{R_L} \cdot \left(4q\,(I_{\mathrm{OLO}} + I_d) + i_{\mathrm{TIA}}^2\right) B, \tag{7}$$

where q is the elementary charge, $I_{\mathrm{OLO}} = \frac{P_{\mathrm{L}}}{2} R_{\mathrm{BPD}} G_{\mathrm{TOLO}}$ is the average photocurrent generated by the OLO in each photodiode of the BPD, I_d is the dark current of each photodiode and i_{TIA} is the equivalent input noise density of the TIA, in $\mathrm{A.Hz}^{-\frac{1}{2}}$. For a matter of simplicity, it is assumed that the average current in each photodiode is approximated by I_{OLO}. As the TIA boosts the power of the output signal the thermal noise generated by the output load can thus be neglected.

The SNR of the output signal is therefore given by

$$\mathrm{SNR}_{\mathrm{out}} = \frac{P_{\mathrm{out}}}{P_{\mathrm{n}}} = \frac{P_{\mathrm{out}}}{P_{\mathrm{n,AE}} + P_{\mathrm{n,OA}} + P_{\mathrm{n,out}}}. \tag{8}$$

In order to assess the relevance of each noise source let us consider a realistic simulation scenario based on the thinned PAA shown in Fig. 3(c) with $N = 1116$ AEs, and also on the scenario presented in [1]. Each uplink user beam with any given color has a bandwidth of $B = 1.25\,\mathrm{GHz}$ [1] and generates an input power of $P_s = -115\,\mathrm{dBW}$ per polarization for each AE. Two different polarizations are assumed, and thus each feed generates two signals. The PBS must thus be subdivided in two identical subsystems, each handling N inputs and outputting $N_B/2 = 130$ beams. The remaining parameters are $P_{\mathrm{L}} = 0.1 \times N = 111.6\,\mathrm{W}$, $\alpha_{\mathrm{F}} = 0.5\,\mathrm{dB}$, $\alpha_{\mathrm{M}} = 12\,\mathrm{dB}$, $\alpha_{\mathrm{LO}} = 15\,\mathrm{dB}$, $\alpha_{s1}^{-1} = 1 - 10^{-2}/\left(P_{\mathrm{L}}\alpha_{s5}^{-1}\right)$, such that the input power at the frequency shifter is of 10 mW, $\alpha_{s2} = 2N$, $\alpha_{s3} = N_B/2$, $\alpha_{s4} = N$, $\alpha_{s5} = N_B$, $G_{\mathrm{OA}} = G_{\mathrm{LOA}} = 20\,\mathrm{dB}$, $G_{\mathrm{OLO}} = 10\,\mathrm{dB}$, $R_{\mathrm{BPD}} = 1\,\mathrm{A\,W}^{-1}$, $R_L = 50\,\Omega$, and $G_{\mathrm{TIA}} = 500\,\mathrm{V\,A}^{-1}$. Regarding noise parameters, let us assume $T_o = 300\,\mathrm{K}$, $T_A = 285\,\mathrm{K}$, $F_{\mathrm{LNA}} = 2.5\,\mathrm{dB}$, $n_{\mathrm{sp,OA}} = n_{\mathrm{sp,LOA}} = 1.58$, which corresponds to a noise figure of about 5 dB, $I_d = 100\,\mathrm{nA}$ and $i_{\mathrm{TIA}} = 40\,\mathrm{pA\,Hz}^{-\frac{1}{2}}$. For a matter of simplicity, each beamforming module has $|w_{bn}|^2 = w_{bn}^2 = -20\,\mathrm{dB}$. Such value models ILs not only from the PBS, but from other components such as couplers, optical amplifiers and BPDs. While the IL of the PBS should depend on N, an IL beyond 20 dB would have a deleterious impact, as it would force the output power of the preceding optical amplifiers to be unfeasibly high.

Figure 7 shows the SNR and P_{out} as a function of G_{LNA} for different noise contributions. As expected, the output signal power is proportional to the gain of the different electrical and OAs. However, it should be noted that G_{LNA} can only be increased up to a limit defined by the half-wave voltage of the EOM. Nonetheless, and considering that each EOM is adapted to an impedance of $50\,\Omega$, the highest considered peak input voltage at the modulator is of 1.7 V, which is lower than the half-wave voltage of state-of-the-art MZMs. In terms of noise, the input RF stages, comprising the AEs and LNAs, handle extremely weak signals, unavoidably adding a significant amount of noise. Hence, the SNR is capped at $\mathrm{SNR}_{\mathrm{max}} = 42.3\,\mathrm{dB}$ due to $P_{\mathrm{n,AE}}$ alone. For low values of G_{LNA} the input power of the OAs becomes too low, thus making optical amplification extremely noisy. In this case the SNR becomes dominated by $P_{\mathrm{n,OA}}$. If the input optical power at the receiver is too low, the SNR becomes dominated by $P_{\mathrm{n,out}}$, which is approximately constant. The SNR may thus be approximated by

$$\mathrm{SNR}_{\mathrm{out}} \approx \frac{P_{\mathrm{out}}}{\max\left\{P_{\mathrm{n,AE}}, P_{\mathrm{n,OA}}, P_{\mathrm{n,out}}\right\}}. \tag{9}$$

6. Power consumption

A simple estimation of the total power consumption can be made by first considering how each active component scales with N and N_B. Taking into account that each AE outputs two signals

Optics EXPRESS

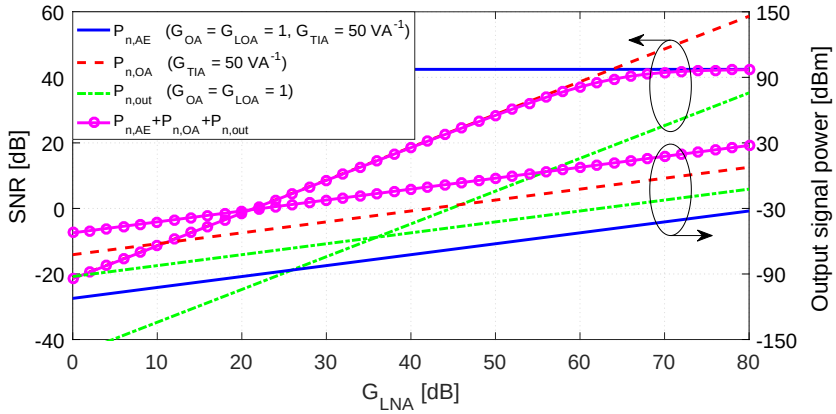

Fig. 7. SNR and P_{out} as a function of G_{LNA} considering different noise contributions. G_{TIA} is set to 50 V A^{-1} when output electrical amplification is not considered such that the TIA is equivalent to a load of 50 Ω. For the contribution of all noise sources (lines with circles) all parameters are quantified according to the described simulation scenario.

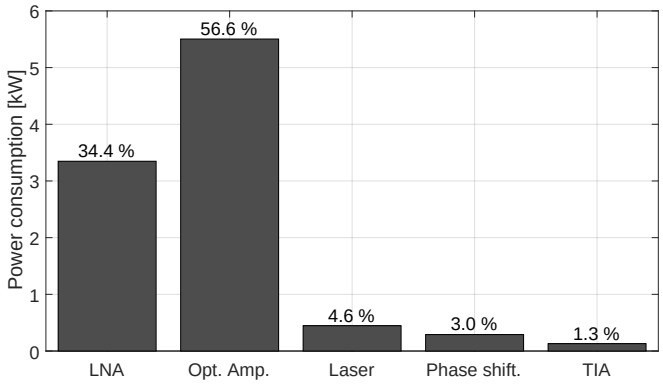

Fig. 8. Power consumption of each kind of component. The percentage of total power consumption is displayed at the top of each bar. Total power consumption is of 9.7 kW.

from each received polarization the number of LNAs is given by $2N$, of OAs is of $2N + 2N_B$, and of TIAs of N_B. According to (1), the PBS has $N \cdot N_B$ phase shifters, assuming that TTD is not used. As for the power consumption required to generate the total laser power, the simplest way is to consider that such power is generated with a given efficiency.

Let us assume $N = 1116$, a laser power of 100 mW per AE, totaling 112 W, and a laser generation efficiency of 25 %. Such a high laser power can be efficiently generated by injection-locking N slave lasers, each with 100 mW of output power, with reference light provided a high-quality master laser source [17]. The power consumption of each LNA, OA, TIA and phase shifter is of 1.5 W, 2 W, 0.5 W and 1 mW, respectively. The power consumption of all devices is shown in Fig. 8.

The majority of power consumption is taken by the LNAs and OAs, totaling 91 %. Given the low power consumption of each phase shifter of 1 mW, the PBS only consumes 3 % of the total power consumption. However, if each phase shifter consumes 10 mW, the power consumed by all phase shifters increases to 23.5 % of the total power consumption, now being on the same level as LNAs.

The reduction of power consumption should focus on three aspects. First, cutting on the number

Optics EXPRESS

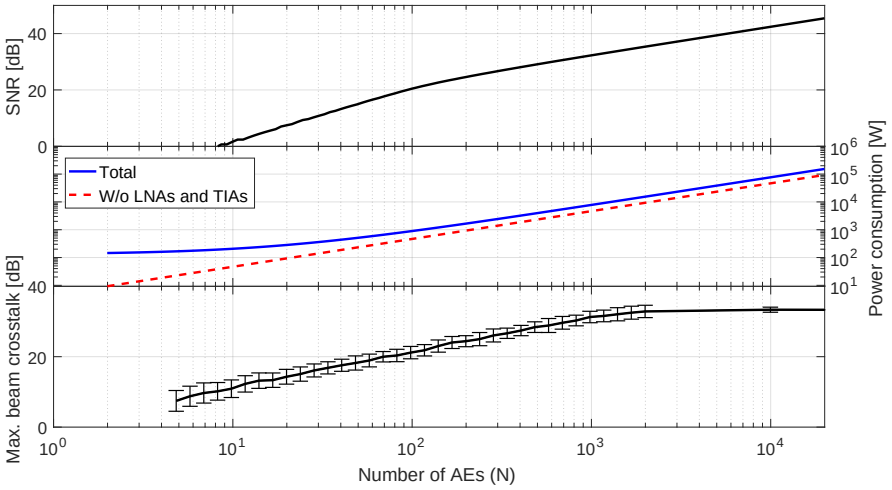

Fig. 9. SNR, power consumption and maximum beam crosstalk as a function of N. The height of the error bars in the bottom plot is given by the standard deviation of the 100 realizations run for each value of N.

of OAs by making dispensable at least one of the three OAs in Fig. 6; second, thinning the array even further such that both the number of LNAs and OAs decreases as well; and third, improve the power efficiency of the LNAs and OAs.

7. End-to-end system dimensioning

The PAA and the PBS should be dimensioned end-to-end such that the target performance is achieved with minimum mass and power consumption. Sections 4 to 6 show that the number of components, and thus mass and power consumption decrease with array thinning, However, array thinning also decreases the SNR, and, due to the limited side lobe suppression in the array factor, enhances beam crosstalk.

Using the tools provided by the last three sections, one can quantify such trade-offs by estimating the SNR, power consumption and beam crosstalk as a function of N. Let us consider the same simulation scenarios as presented above, and also the following. For estimating beam crosstalk, the reference beam is the center beam, located at $(\alpha_T, \beta_T) = (0, 0)$. Other than the center beam, a total of 50 beams with same polarization and frequency are considered, within a span of $\pm 3.57° \times \pm 0.42°$. For any given value of N, the estimated crosstalk depends on how the array is thinned. In order to estimate a crosstalk interval for each value of N, 100 realizations are run, each of which has a random selection of N AEs out of the 19927 AEs of the filled array. The presented crosstalk corresponds to the maximum crosstalk produced by any given beam. In order to minimize power consumption, it is assumed that $G_{\mathrm{OLO}} = G_{\mathrm{LOA}} = 1$, thus dispensing these OAs. The number of OAs then becomes $2N$. In order to compensate for such lack of amplification, let us assume $G_{\mathrm{OA}} = 40\,\mathrm{dB}$, $G_{\mathrm{LNA}} = 45\,\mathrm{dB}$, given that such is the typical maximum gain of commercially available Ka band LNAs, and $\alpha_{s1}^{-1} = \max\left\{1 - 1.5 \times 10^{-2}/\left(P_{\mathrm{L}}\alpha_{s5}^{-1}\right), 0.5\right\}$, such that the input power at the frequency shifter increases to 15 mW as long as at least half the laser power goes to the EOMs.

As shown in Fig. 9, all three figures of merit increase smoothly with N. While a maximum SNR of 45.4 dB can be obtained for the highest number of AEs, such comes at the cost of consuming over 10 kW of power. In practice, power consumption limits the number of AEs to about 100 [13]. For such a number, the proposed system achieves a maximum beam crosstalk

Optics EXPRESS

of 21 dB, SNR of 20 dB, total power consumption of 896 W, and power consumption of optical devices, i.e., excluding LNAs and TIA, of 466 W. The breakdown of the power consumption is similar to Fig. 8, but with the OAs taking 12 % less power, which goes to the TIAs.

The analysis above assumes all beams as squint-free. However, in the considered scenario [1], each beam has a maximum spectral width up to 1.25 GHz. As shown in Fig. 5(b), while 66.6 % of the beams with such a spectral width may be assumed squint-free without requiring TTD beamforming, such may not be the case for the remaining beams. Introducing TTD beamforming requires at least one delay line per AE for each beamforming stage enabling TTD beamforming. Thus, the number of required delay lines lies between 33.3 % and 100 % of $N \cdot N_B$. Adding these many delay lines has an impact in power consumption and footprint. In terms of power consumption, the impact depends on the tuning mechanism of the delay lines. Assuming that all delays are TODLs requiring one phase shifter for delay tuning, the total number of phase shifters may increase up to $2 \times N \cdot N_B$, thus doubling the power consumption of phase shifters to 52 W. Such increase in power is negligible when compared with the 400 W consumed by OAs. The increase in footprint of the PBS depends both on the number of delay lines and of required maximum delay, which is of 660 ps for the outermost AEs for $(\alpha_T, \beta_T) = (3.5°, 2.0°)$. For such angles, the cumulative absolute delay required by 100 AEs is of about 30 ns. Hence, for a fully flexible PBS with any of the $N_B = 260$ beamforming stages capable of providing TTD beamforming to any beam, a total cumulative absolute delay of 7.8 µs is required. Even for a single beamforming stage, a delay of 30 ns is too long to be implemented within a silicon photonic integrated circuit (PIC) [18], as it would require a total waveguide length of about 2.5 m.

8. Conclusions

In this paper, a multi-beam PBS fed by a PAA for a communications satellite receiver was proposed, modeled and dimensioned with the objective of quantifying the trade-off between performance, mass and power consumption. The proposed receiver uses a single wavelength and resorts to heterodyne detection to frequency-downconvert the retrieved beams, thus being as close as possible to the original RF heterodyne receiver. However, given that the optical wavelength is about 5000 times shorter than the RF wavelength, the PBS can be miniaturized by such factor, thus reducing mass.

System modeling demonstrates that complexity, quantified in number of AEs, and thus power consumption, can be decreased at the cost of lower SNR and stronger beam crosstalk, however without compromising the beam width. End-to-end system dimensioning shows that for the typical number of AEs, i.e., $N = 100$, an SNR and beam crosstalk on the order of 20 dB are achievable in a realistic scenario with sub-kilowatt power consumption. Leaving the LNAs aside, introducing photonics takes about 70 % of such power consumption, most of it going to optical amplification. Interestingly, the PBS only consumes about 3 % of such power. This shows that once photonics is introduced for mere transportation or frequency downconversion of signals, adding a fully-flexible multi-beam PBS produces a negligible impact on power consumption. Furthermore, such flexibility obviates the need for a beam switch interconnecting receiving and transmitting stages. Such conclusion shows that photonics is indeed an attractive solution for the ultimate goal of achieving a software-defined coverage.

The implementation of the proposed system has three main challenges. First, even with as few as $N = 100$ AEs, the number of required phase shifters is of at least 100 per beam, totaling 26×10^3 phase shifters. While the most compact implementation of the PBS is within a single PIC, integrating so many phase shifters together with all optical couplers is unfeasible. A more manageable and modular approach thus is to use one PIC per beam, i.e., to separately implement N_B single-beam beamformers. Second, given that at least one beam may require TTD beamforming, there is a need of choosing suitable delay lines, and also of where to integrate them. The use of simple non-tunable delay lines results in a squint-free but inflexible PBS, in

Optics EXPRESS

which any given beamforming stage may only address a limited set of beams. Hence, there is a trade-off between PBS flexibility versus use and tunability of the delay lines. Concerning where to integrate the delay lines, the approach of using N_B single-beam beamformers is again favorable. Modular delay lines can be placed before each beamforming stage, leaving the integration of delay lines within a beamforming stage no longer mandatory. Third, the relative phases among the N input signals that are processed to yield one output beam need to be monitored such that w_{bn} can be tuned and kept stable against slow but unavoidable path length drifts. This task requires a phase-locked loop monitoring and control system that, albeit slow, needs to control the phase of $N \times N_B$ signals [19].

Funding

FCT/MEC through national funds and when applicable co-funded by FEDER – PT2020 partnership agreement under the project UID/EEA/50008/2013; European Commission-funded project BEACON (FP7-SPACE-2013-1-607401).